



Al-Rafidain Journal of Engineering Sciences

Journal homepage <https://rjes.iq/index.php/rjes>

ISSN 3005-3153 (Online)



Thermal Effects on Kinetics and Catalytic Efficiency of LaNiMnO_3 in Methane Dry Reforming

Halah A. Ramadhan¹, Maha Al-Ali²

¹Department of Chemical Engineering/College of Engineering /Tikrit University/ Tikrit/ Iraq

²Department of Oil and Gas Refining/College of Petroleum Process Engineering/ Tikrit University/ Tikrit/ Iraq

ARTICLE INFO

Article history:

Received 16 September 2024
 Revised 17 September 2024
 Accepted 01 October 2024
 Available online 17 October 2024

Keywords:

Kinetics
 Perovskite catalyst
 Power law model
 sol-gel method
 syngas

ABSTRACT

In this work a kinetic study over LaNiMnO_3 perovskite catalyst in the catalytic dry reforming of methane is investigated. The novel catalyst was prepared using the sol-gel method. The performance experiments were conducted in a fixed bed reactor at temperatures ranging from 500 to 800 °C with feed ratio of ($\text{CH}_4:\text{CO}_2:\text{N}_2=1:1:2$) ml/min. The temperature effect and time on the catalyst activity and stability were studied. As well as the activation energy and H_2/CO ratio are estimated. The reaction rate equation of catalytic dry reforming of methane was investigated by applying the power law model assuming isothermal reaction and the pressure drop was ignored. The catalyst showed 67.43% and 62.2% conversion rates in terms of CH_4 and CO_2 at 800 °C, respectively. The kinetic parameters (rate constants and orders) were determined and the activation energy equaled to 30.728 kJ/mol. The catalyst showed H_2/CO ratio higher than 1, due to the occurrence of Boudouard side reaction. To conclude, this study develops new catalyst with good catalytic performance and the rate model was successfully investigated.

1. Introduction

The significant increase in global energy demand in the past few years has resulted in an extensive use of traditional fossil fuels and an excess of greenhouse gas emissions [1]. These gases, mainly carbon dioxide and methane, are constantly released into the atmosphere. These two gases have been identified as the primary contributors of global warming and, thus,

climate change [2]. Catalytic dry reforming of methane (CDRM) technology converts methane (CH_4) and carbon dioxide (CO_2) into syngas with an H_2/CO ratio of 1. The resultant syngas is well-suited for subsequent Fischer-Tropsch (F-T) synthesis of long-chain hydrocarbons and hydroxyl synthesis of oxygenated chemicals [3]. For over 30 years, researchers have extensively examined the DRM reaction using various catalysts, including both noble and non-noble

* Corresponding author E-mail address: halah.a.ramadhan42116@st.tu.edu.iq
<https://doi.org/10.61268/0fcxf449>

This work is an open-access article distributed under a CC BY license (Creative Commons Attribution 4.0 International) under

<https://creativecommons.org/licenses/by-nc-sa/4.0/> 

metals. Among them, nickel-based catalysts are widely studied and considered attractive candidates for DRM due to their comparable activity to noble metals and low cost [4]. Catalysts offer an alternative route to minimize activation energy, lowering the energy required to attain the transition state. Catalysts can significantly reduce the reaction temperature of DRM. Noble metal catalysts such as Pd, Ru, and Rh have been studied for their excellent anti-coking properties and stability. However, limited resources and expensive prices make it unsuitable for industrial development [5]. On the contrary, Ni-based catalysts have gained a lot of interest due to their abundant resources and strong initial activity. However, the key problems for Ni-based catalysts are metal sintering and carbon deposition on the catalyst surface, which will reduce catalytic activity, service life, and possibly lead to deactivation of the catalyst [6]. To solve these challenges, perovskite oxides with excellent thermal stability and low cost are used as catalyst precursors or supports to improve metal-support interaction (MSI) and surface characteristics. Furthermore, the perovskite structure can be partially replaced by different cations, resulting in a shift in oxidation state and increasing redox characteristics [7]. A lot of researchers studied the performance of perovskite catalysts in the catalytic dry reforming of methane process, for example, Roman et al. [8] synthesized $\text{La}_2\text{Ce}_2\text{O}_7$ and LaNiO_3 mixed oxides by two methods of preparation, modified Pechini and hydrothermal methods. The results they got showed that the sample prepared by hydrothermal method exhibited the highest conversions and yield. This performance can be attributed to the higher number of basic sites, oxygen vacancies and stronger interactions between nickel and cerium.

Another work for De lira lima et al. [9] they aimed to synthesized $\text{LaNi}_{1-x}\text{Co}_x\text{O}_3$ ($x = 0.0, 0.1, 0.2, 0.5$ and 1.0) perovskite-type oxides, in two ways pure and incorporated into silica. They applied them as catalytic precursors in the catalytic dry reforming of methane, either pure or mixed with silica. They obtained that the substitution of Co for Ni resulted in a drop in catalytic performance, revealing Ni's crucial in these materials' catalytic activity. The LaNiO_3 sample demonstrated great stability on stream for 24 hours. CO_2 conversion was consistently higher than that of CH_4 . All samples had an H_2/CO ratio less than one, indicating the occurrence of side reactions such as reverse water gas shift reaction RWGS. A mechanical combination of perovskites and non-porous silica resulted in an increase in CH_4 and CO_2 conversions, as well as the H_2/CO ratio.

Therefore, this work focuses on using LaNiMnO_3 perovskite oxide catalyst in the CDRM reaction. In this work, LaNiMnO_3 synthesized by sol-gel method, and employed as catalyst precursor in the CDRM reaction to increase the reaction conversion rate and yield of hydrogen gas, and it was chosen because it is less expensive, more readily available, and better suited for heating than other catalysts. The chemical kinetics of this reaction with our prepared catalyst are examined, and the reaction rate and constants are determined. The minimal amount of energy needed for the CDRM reaction is determined by calculating the reaction's activation energy. Thus, the objective of this study is to investigate the kinetics of the CDRM reaction in order to describe system performance using LaNiMnO_3 perovskite oxide catalyst under established operating conditions in order to produce a renewable energy source with appropriate conversion.

2. Methodology

2.1: Method of preparation:

LaNiMnO₃ perovskite catalyst was prepared by the sol-gel method [10]. Lanthanum nitrate hexahydrate (La(NO₃)₂.6H₂O) with a purity of 99% was purchased from Gainland Chemical Company (GCC), Nickel nitrate hexahydrate (Ni(NO₃)₂.6H₂O) and Manganese nitrate hydrate (MnN₂O₆.xH₂O) were purchased from Sigma Aldrich company, both with a purity of 98%, the nitrates were used as the active materials in the catalyst preparation. Citric acid was used as co-crystallization emulsifier. A stoichiometric amounts of the nitrates were dissolved in 50 ml of deionized water, and a 3g of citric acid were added to the solution to obtain the perovskite oxides materials. The solution was heated at 80 °C for 6 hrs on a continuous stirring until it becomes a green gel. To remove the residual moisture, the resulted gel dried in the oven for 14 hr at a temperature of 110 °C, and a powder was obtained. Lastly, the powder was calcined in a tubular furnace for 5 hrs at 800 °C.

2.2: Reaction set up:

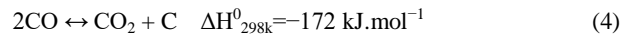
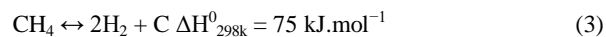
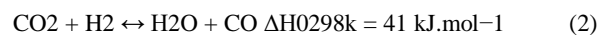
The reaction carried at a fixed bed reactor with the specifications of 40 cm height, 10 mm outside diameter, and 6 mm inside diameter. The reactor operating at a maximal temperature of 850 °C with a rate of 15 °C/min. The reactor consisted of a stainless-steel mesh cup ranging in size from 2 to 5 mm. It used to hold the catalyst powder (100 mg) and was placed in the center of the reactor bed. Firstly, a 50 ml/min flow of H₂ gas was opened for 30 min at 800 °C to activate the catalyst powder before the reaction started. Secondly, a mixture of CH₄, CO₂, and N₂ gases were presented at a 60 ml/min flow rate at a ratio 30:15:15 ml/min of

N₂:CH₄:CO₂, the pressure was 1 atm. The gases flow was controlled by individual flowmeters for each gas. The experiments were conducted at four temperatures 500, 600, 700, and 800 °C. The resultant gas was obtained from the reactor bed and constructed with nylon balls before being analyzed in a gas chromatograph device (GC) to determine the rate of conversion of methane and carbon dioxide gas.

The same procedure was repeated, and product samples were collected one hour after the reaction, to be analyzed. After a second cleaning, the reactor was refilled with catalyst powder. Gases were injected into the reactor in the same quantities as in step one, while maintaining a constant temperature of 800 °C for 1, 2, 3, 4, 5, 6, 7, 8, 9, 10, and 15 hours. The data was analyzed by measuring the percentage of methane gas remained after the process and establishing its conversion rates.

2.3. Kinetic measurements

Kinetic studies for the catalytic reforming reaction of CH₄ with CO₂ under different conditions were conducted in the same reactor system. The kinetic models in the literature can be divided into three broad classes. a) Power law models, b) Model-based pathway analysis, and c) Elementary kinetic (micro-kinetic) models [11]. In this study, the kinetics of the CDRM reaction are investigated based on power law model. Generally, the CDRM reaction Eq. (1), proceeds several reactions Eqs. (2)-(4), these reactions actually are undesirable [12].

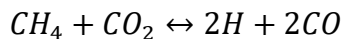


The CDRM reaction according to Eq. (1) is a promising method, with the ability to directly valorize CO₂ as a feedstock. At the high temperatures required for thermal CDRM reaction and in addition to CH₄ pyrolysis, when additional species such CO₂ and H₂ are present in the feed, reverse water gas shift reaction (RWGS) Eq. (2) becomes significant. This endothermic process, which has no direct CO₂ emissions, involves the decomposing of CH₄, leading to in the creation of H₂ and the extraction of solid carbon according to Eq. (3). An increase in pressure related with the Boudouard reaction Eq. (4) causes an increase in carbon deposition [12]. The stoichiometric equation Eq. (5) was used to compute the measured selectivity H₂/CO ratios. This reaction suggests that the instantaneous occurrence of the (RWGS) reaction has an impact on the CDRM reaction.

$$H_2/CO = (3 - \frac{r_{CO_2}}{r_{CH_4}}) / (1 + \frac{r_{CO_2}}{r_{CH_4}}) \quad (5)$$

where r_{CO_2} and r_{CH_4} are the experimental conversion rates of CH₄ and CO₂, respectively [2]. The differential method of analysis was applied to obtain the rate equation with the rate constant and the orders of reaction species [13]. The differential method helps to identify contradictions in experimental data. To illustrate the approach employed in the differential method of analysis, we consider isothermal reaction with negligible pressure drop, as well as the concentration of component (A) measured as a function of time [13].

The reaction equation:



Represented by:



$$\frac{-r_A}{a} = \frac{-r_B}{b} = \frac{r_C}{c} = \frac{r_D}{d}$$

The overall rate law of reaction:

$$-r'_a = k_1 C_A^\alpha C_B^\beta - k_{-1} C_C^\gamma C_D^\sigma \quad (7)$$

The forward reaction:

$$-r'_f = k_1 C_A^\alpha C_B^\beta \quad (8)$$

The backward reaction:

$$-r'_{-f} = k_{-1} C_C^\gamma C_D^\sigma \quad (9)$$

For the forward reaction Eq.(8) we considered C_B constant (C_B = C_{B0}), thus our equation becomes:

$$-r'_f = (k_1 C_{B0}^\beta) C_A^\alpha \quad (10)$$

(k₁C_{B0}^β) = K, therefor the forward rate equation:

$$-r'_f = K C_A^\alpha \quad (11)$$

taking the natural log of both sides of Eq. (11)

$$\ln(-r'_f) = \ln(K) + \alpha \ln C_A \quad (12)$$

In which $-r'_f = r'_c = 2(-r'_A) = 2(-r'_B)$
 $-r'_A$ can be calculated by:

$$-r'_A = \frac{F_{A0} X}{\Delta W} \quad (13)$$

X represents the conversion rate of A.

$$F_{A0} = \frac{v_A \rho_A}{MW} \quad (14)$$

$$C_A = C_{A0} \frac{(1-x)}{(1+\epsilon x)} \quad (15)$$

$$C_B = C_{A0} \frac{(\theta_B - \frac{b}{a}x)}{(1+\epsilon x)} \quad (16)$$

$$C_C = C_{A0} \frac{(\theta_C + \frac{c}{a}x)}{(1+\varepsilon x)} \quad (17)$$

and equals to C_D

$$\theta_i = \frac{F_{i0}}{F_{A0}} \quad (18)$$

$$F_{A0} = 0.0368 \frac{\text{mol}}{\text{hr}},$$

$$F_{B0} = 0.0367 \frac{\text{mol}}{\text{hr}},$$

$$F_{C0} = 0 = F_{D0}$$

$$\therefore \theta_B = 0.997, \theta_C = \theta_D = 0$$

$$\varepsilon = y_{A0} \delta \quad (19)$$

$$\delta = \left(\frac{d}{a} + \frac{c}{a}\right) - \left(\frac{b}{a} + \frac{a}{a}\right) = \frac{2}{1} + \frac{2}{1} - \frac{1}{1} - \frac{1}{1} = 2$$

$$\therefore \varepsilon = 0.5 * 2 = 1$$

3. Results and discussion

3.1: Temperature effect on catalytic activity

In this section we represent the temperature effect on the reactants activity. The experiments were conducted at four temperatures (500, 600, 700, and 800) °C through constant time intervals. Fig. 1 represents the conversions raise with temperature. The conversions of CH₄ and CO₂ at the first temperature 500 °C are 17.26 and 13.71%, respectively, in which it considered to be low. But with increasing the temperature. temperature to 600, 700 and 800 °C, the rates of CH₄ and CO₂ conversion increased to 29.65 and 25.96%, 48.19 and 44.49%, and 67.43 and 62.2%, respectively. From this behavior we can say that, the conversions increased with increasing of reaction temperature. This can be explained through the fact of that the CDRM reaction is endothermic reaction, means it

requires elevated temperatures. Similar results were obtained by several researchers for example, Shahnazi et al. [14] synthesized mesoporous LaNi_{1-x}Mn_xO₃ (0<x<1) perovskite catalysts by ultrasonic spray pyrolysis method. They applied them in the dry reforming reaction at the temperature range of (600-800) °C, they showed good catalytic activity with high conversion rates of CH₄ and CO₂, the tests showed that they raised from 55% and 50% at 600°C to 90% and 83% at 800°C, respectively. Another study for Wei et al. [15] they prepared La_{0.8-x}Sr_xCr_{0.85}Ni_{0.15}O₃ (x = 0, 0.1, 0.2 and 0.3) in the reduced forms (R-80, R-71, R-62, R-53) catalysts. They applied them in the CDRM reaction at the temperature range of (600-800) °C they obtained that R-62 form exhibited the highest conversion 92% at 800 °C, the conversion was increased with temperature increasing.

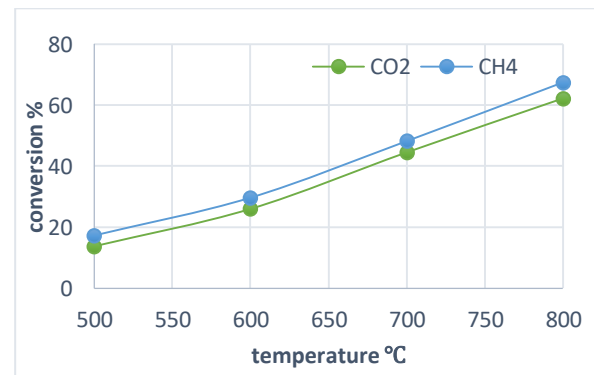


Fig.1: CH₄ and CO₂ conversions after 1 hr of reaction.

3.2: Long term Stability test

The stability test for LaNiMnO₃ catalyst was performed in the reactor at 800 °C for 15 hrs with an interval of 1 hr. Fig. 2 represents the stability of CH₄ and CO₂ conversion rates with time.

The figure shows that the conversion rates decreased with time, CH₄ and CO₂ conversions decreased from 67.43% to 50.21% and 62.2% to 48.36%, respectively, after 15 hrs of reaction. This decrease may be attributed to carbon formation [16]. However, LaNiMnO₃ exhibited good catalytic stability in comparison to other Ni-based catalysts, for example, Newnham et al. [17] prepared 10%Ni/γ-Al₂O₃ catalyst by the co-precipitation method, and applied it in the CDRM reaction, the catalyst exhibited a significant loss in activity only after 4 hrs of reaction. Another study for jeong et al. [18] they studied the effect of inserting a promoter K into Ni/HY catalyst, the Ni-K/HY catalyst showed severe coke formation after 24 hrs of reaction in which CH₄ conversion decreased from 97% to 0%.

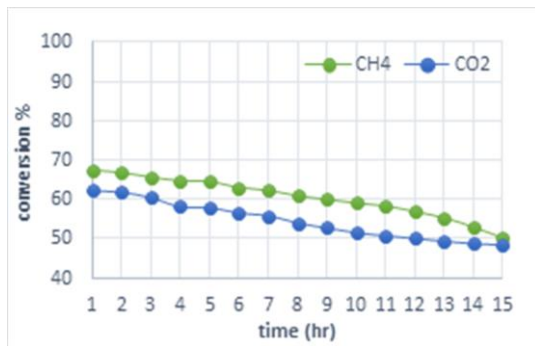


Fig.2: Conversion changes of CH₄ and CO₂ versus time at 800°C.

3.3: Kinetic calculations

The kinetics of CH₄ reforming with CO₂ over LaNiMnO₃ catalyst was determined at 800°C. The reaction rate obtained by using the experimental data, and the kinetic parameters (k₁, k₋₁, K, α, β, and γ) were calculated.

To determine the reaction constant and the orders of components (A, B, and C) from the experimental data, we start with Eq. (12)

$$\therefore -r'_f = r'_c = 2(-r'_A)$$

Eq.(12) becomes

$$\ln(r'_c) = \ln(K) + \alpha \ln C_A \tag{20}$$

$-r'_A$ calculated by Eq. (13), $(-r'_A = \frac{F_{A0} X}{\Delta W})$

From the experimental data a plot of ln(-r_A) versus ln(C_A) was established to calculate K and α.

From Fig. 3 we got the slope, α = 0.5417, and the intercept represents ln(K) and equal to -3.3086 thus K = 0.3656 * 10⁻¹ mol. l⁻² gmcat⁻¹ h⁻¹

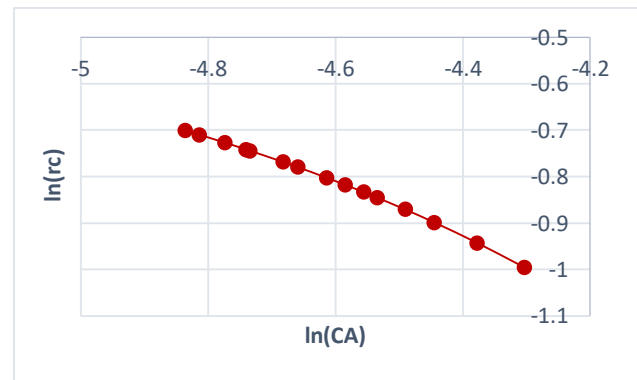


Fig. 3: Plotting of Ln(rc) versus Ln(CA)

To calculate the order of C_B, from Eq. (8)

$$\begin{aligned} -r'_B &= k C_B^\beta \\ \therefore r'_c &= 2(-r'_A) = 2(-r'_B) \\ \therefore \ln(r'_c) &= \ln(k) + \beta \ln C_B \end{aligned} \tag{21}$$

Experimental data k shown in Fig. 4.

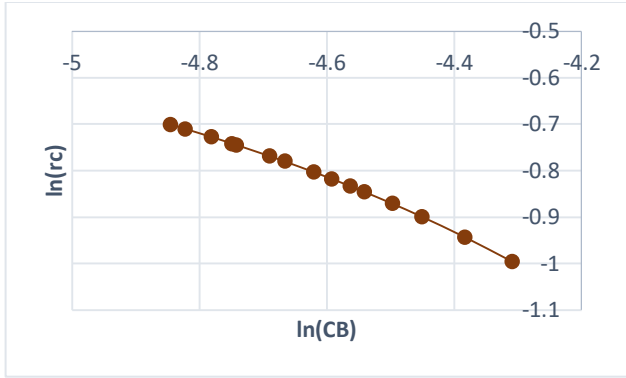


Fig. 4: Plotting of Ln(rc) versus Ln(CB)

The slope $\beta=0.5834$ and the intercept $\ln(k)=-3.2976$, therefor $k=0.3697 \cdot 10^{-1} \text{ mol. l}^{-2} \text{ gmcat}^{-1} \text{ h}^{-1}$, from β and C_{B0} we can calculate k_1 :

$$(k_1 C_{B0}^\beta) = K \rightarrow k_1 = \frac{K}{C_{B0}^\beta} = \frac{0.03656}{0.0407^{0.5834}} =$$

$$0.20496 \text{ mol.l}^{-2} \text{ gmcat}^{-1} \text{ h}^{-1}$$

Thus $-r'_f = k_1 C_A^\alpha C_B^\beta$ becomes

$$-r'_f = 2.049 \cdot 10^{-1} C_A^{0.5417} C_B^{0.5834} \quad (22)$$

For backward reaction:

$$-r'_{-f} = k_{-1} C_C^\gamma C_D^\sigma$$

the concentration of component C equals D [13], since the product ratio (H_2/CO) from the CDRM is equals to unity. Thus the backward reaction is a function of C_C only.

$$-r'_{-f} = k_{-1} C_C^\gamma \rightarrow -r'_c = k_{-1} C_C^\gamma$$

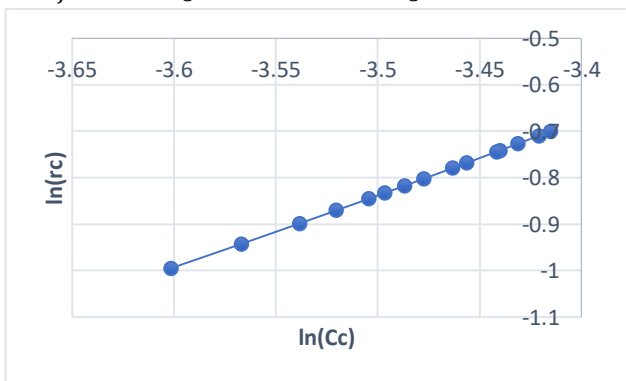


Fig. 5: Plotting of Ln(rc) versus Ln(Cc)

From Fig. 5 we obtained the slope, $\gamma = 1.5878$, and the intercept represents $\ln(k_{-1})$ and equal to 3.7202 thus $k_{-1} = 0.4127 \cdot 10^2 \text{ mol. l}^{-2} \text{ gmcat}^{-1} \text{ h}^{-1}$

$$-r'_{-f} = 0.4127 \cdot 10^2 C_C^{1.5878} \quad (23)$$

Therefor the overall rate equation

$$-r'_a = k_1 C_A^\alpha C_B^\beta - k_{-1} C_C^\gamma$$

can be written as:

$$-r'_a = 0.20496 C_A^{0.5417} C_B^{0.5834} - 0.4127 \cdot 10^2 C_C^{1.5878} \quad (24)$$

3.4 . H2/CO ratio

The selectivity of H_2/CO was calculated by Eq. (5). Fig. 6 shows the H_2/CO ratio during 15 hrs of reaction, the H_2/CO values are greater than 1, indicating that the Boudouard reaction is the main side reaction [19].

From Fig. 6 we observed H_2/CO ratio is 1.08 within the first hour of reaction and reached 1.139 after 11 hrs of reaction, then it decreased to 1.03 after 15 hrs of reaction. Similar results were obtained by Al-Otaibi et al. [20] they got H_2/CO ratio values greater than 1 and they suggested that this behavior indicates that the methane decomposition led to H_2 production. Another work for Kim et al. [21] they also obtained H_2/CO ratio higher than 1 during the CDRM reaction, they indicated that these high values of H_2/CO ratio due to methane cracking reaction, Boudouard reaction and RWGS reaction.

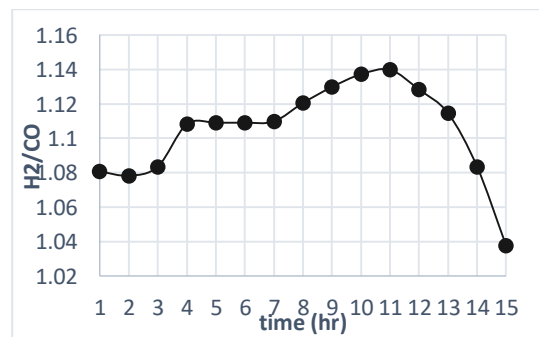


Fig. 6: H_2/CO ratio of CDRM reaction with time.

3.5. Activation energy calculations

Activation energy is a key kinetic measurement used to rate reactions for the mechanism development and chemical reaction modelling. Efficient activation energy estimation is crucial for accurately predicting kinetics [22]. It is defined as the minimum amount of energy needed to start a chemical reaction [23]. As a reaction advances over time, graphing the reaction's energy can reflect the changes happening during the reaction. This makes it possible to collect important information on the reaction rate and how it changes with temperature. The activation energy was calculated by using the Arrhenius equation

$$k = A * \exp \frac{-EA}{RT} \quad (25)$$

where (A) represents the pre-exponential factor, (EA) is the activation energy, (R) is the ideal gas constant, and (T) is the absolute temperature in kelvin [24]. The Arrhenius equation states that the apparent activation energy is determined by the slope of the logarithm of reaction rates versus inverse of reaction temperature [25].

The experiments used to determine the activation energy were conducted at atmospheric pressure and temperatures ranging from 500-800 °C, with a step of 100 °C, using 100 mg of catalyst powder, starting with Eq. (8) and Eq. (13) to obtain the k_1 values and calculate the rate at each reaction temperature, respectively.

$$\ln k_1 = -\frac{EA}{R} \frac{1}{T} + \ln A \quad (26)$$

From Fig. 7 we obtained the slope which represents $(-\frac{EA}{R}) = -3696$ thus $EA=30.728$ kJ/mol and the intercept represents $\ln A=8.4681$ therefor $A=4760.5$. A comparable result was obtained by Khoja et al. [26] they conducted a study on catalytic dry reforming of methane over La_2O_3 co-supported $\text{Ni/MgAl}_2\text{O}_4$ catalyst by using the modified power law model. The activation energy they found for CH_4 dissociation was 32.6 kJ/mol. Higher values for EA could be obtained by other studies for example, Pino et al. [27] studied the kinetic behavior of $\text{Ce}_{0.7}\text{La}_{0.2}\text{Ni}_{0.1}\text{O}_{2-\delta}$ catalyst in the CDRM reaction. The activation energy for the CH_4 consumption from the power law model was 91.5 kJ/mol.

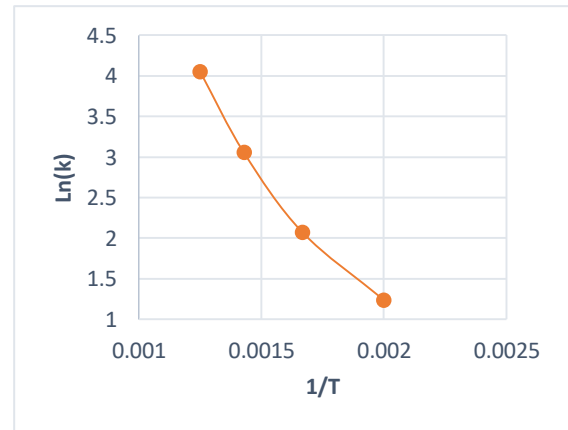


Fig. 7: Plotting $\ln(k_1)$ versus $1/T$.

Table. 1: Conversion Rates of CH₄, concentrations of A and B components, rate of reaction and k1 values at different temperatures.

Temperature (°C)	Conversion	C _A (mol/L)	C _B (mol/L)	-r _A (mol.gm _{cat} ⁻¹ .h ⁻¹)	k1 (mol.L ⁻² .gm _{cat} ⁻¹ .h ⁻¹)
500	0.17262	0.0287	0.0286	0.06352	3.4467
600	0.2965	0.0221	0.022	0.10911	7.9583
700	0.48192	0.0143	0.0141	0.17735	21.2309
800	0.6743	0.0079	0.0078	0.24814	57.5646

4. Conclusions

Power law kinetic model for the overall rate of CDRM reaction is established in terms of CH₄ and CO₂ concentrations. LaNiMnO₃ perovskite catalyst was successfully prepared by the sol-gel method of preparation. The conversion rates of reactants increased with temperature increasing, the higher conversions 67.43% and 62.2% for CH₄ and CO₂, respectively, were at 800 °C. The H₂/CO values were greater than 1 during the 15 hrs of reaction, indicating that the Boudouard reaction is the main side reaction. The minimal energy required for the CDRM reaction was 30.728 kJ/mol. The overall rate of the CDRM reaction can be represented as follows: $-r'_a = 0.20496 C_A^{0.5417} C_B^{0.5834} - 0.4127 * 10^2 C_C^{1.5878}$

Acknowledgment

The authors are grateful to the Chemical Engineering Department, College of Engineering, and the Oil and Gas Refining Department, College of Petroleum Process Engineering, Tikrit University, for granting access to their laboratories. We admire the work of the technical staff of the Petroleum Research and Development Center, and Alkhora nano lab

at Alkhora Company, in Baghdad, Iraq. Also, thanks to Alfaisal Aljbory for his assistance.

References

- [1] Z. Wang *et al.*, "Insight into the activity of Ni-based thermal catalysts for dry reforming of methane," *Journal of Materials Chemistry A*, 2024.
- [2] M. Al-Ali, A. Aljbory, and G. H. Abdullah, "Kinetic Analysis of Catalytic Dry Reforming of Methane Using Ni-ZrO₂/MCM-41 Catalyst," *Tikrit Journal of Engineering Sciences*, vol. 31, no. 1, pp. 236-250, 2024.
- [3] D. Cao *et al.*, "Dry reforming of methane by La₂NiO₄ perovskite oxide: B-site substitution improving reactivity and stability," *Chemical Engineering Journal*, vol. 482, p. 148701, 2024.
- [4] Q. Zhang, M. Akri, Y. Yang, and B. Qiao, "Atomically dispersed metals as potential coke-resistant catalysts for dry reforming of methane," *Cell Reports Physical Science*, vol. 4, no. 3, 2023.
- [5] Y. Zhang *et al.*, "Dry reforming of methane over Ni/SiO₂ catalysts: Role of support structure properties," *Fuel*, vol. 340, p. 127490, 2023.
- [6] Y. Mao, L. Zhang, X. Zheng, W. Liu, Z. Cao, and H. Peng, "Coke-resistance over Rh-Ni bimetallic catalyst for low temperature dry reforming of methane," *International Journal of Hydrogen Energy*, vol. 48, no. 37, pp. 13890-13901, 2023.
- [7] S. Deng, Y. Lei, Y. Deng, Y. Lai, and X. Gao, "Recent advances in the application of perovskite catalysts in the dry reforming of methane," *Catalysis Research*, vol. 2, no. 2, pp. 1-11, 2022.

- [8] A. P. Ramon *et al.*, "In situ study of low-temperature dry reforming of methane over La₂Ce₂O₇ and LaNiO₃ mixed oxides," *Applied Catalysis B: Environmental*, vol. 315, p. 121528, 2022.
- [9] D. C. de Lira Lima *et al.*, "Study of LaNi_{1-x}Co_xO₃ perovskites-type oxides either pure or mixed with SiO₂ as catalytic precursors applied in CH₄ dry-reforming," *Catalysis Letters*, vol. 153, no. 7, pp. 2137-2148, 2023.
- [10] D. Navas, S. Fuentes, A. Castro-Alvarez, and E. Chavez-Angel, "Review on sol-gel synthesis of perovskite and oxide nanomaterials," *Gels*, vol. 7, no. 4, p. 275, 2021.
- [11] P. V. Ponugoti and V. M. Janardhanan, "Mechanistic kinetic model for biogas dry reforming," *Industrial & Engineering Chemistry Research*, vol. 59, no. 33, pp. 14737-14746, 2020.
- [12] M. Mokashi *et al.*, "Kinetics of thermal dry reforming of methane for syngas production and solid carbon capture," *Reaction Chemistry & Engineering*, 2024.
- [13] H. Fogler, "Elements of chemical reaction engineering, 3rd," ed: Prentice Hall International, Inc, New Jersey, 1999.
- [14] A. Shahnazi and S. Firoozi, "Improving the catalytic performance of LaNiO₃ perovskite by manganese substitution via ultrasonic spray pyrolysis for dry reforming of methane," *Journal of CO₂ Utilization*, vol. 45, p. 101455, 2021.
- [15] T. Wei, L. Jia, J.-L. Luo, B. Chi, J. Pu, and J. Li, "CO₂ dry reforming of CH₄ with Sr and Ni co-doped LaCrO₃ perovskite catalysts," *Applied Surface Science*, vol. 506, p. 144699, 2020.
- [16] N. Ahmad, F. Alharthi, M. Alam, R. Wahab, S. Manoharadas, and B. Alrayes, "Syngas production via CO₂ reforming of methane over SrNiO₃ and CeNiO₃ perovskites," *Energies*, vol. 14, no. 10, p. 2928, 2021.
- [17] J. Newnham, K. Mantri, M. H. Amin, J. Tardio, and S. K. Bhargava, "Highly stable and active Ni-mesoporous alumina catalysts for dry reforming of methane," *International journal of hydrogen energy*, vol. 37, no. 2, pp. 1454-1464, 2012.
- [18] H. Jeong, K. I. Kim, D. Kim, and I. K. Song, "Effect of promoters in the methane reforming with carbon dioxide to synthesis gas over Ni/HY catalysts," *Journal of Molecular Catalysis A: Chemical*, vol. 246, no. 1-2, pp. 43-48, 2006.
- [19] M. S. Lanre *et al.*, "Modification of CeNiO₃. 9ZrO₃ perovskite catalyst by partially substituting yttrium with zirconia in dry reforming of methane," *Materials*, vol. 15, no. 10, p. 3564, 2022.
- [20] F. Al-Otaibi, H. Xiao, A. S. Berrouk, and K. Polychronopoulou, "Numerical study of dry reforming of methane in packed and fluidized beds: effects of key operating parameters," *ChemEngineering*, vol. 7, no. 3, p. 57, 2023.
- [21] W. Y. Kim, J. S. Jang, E. C. Ra, K. Y. Kim, E. H. Kim, and J. S. Lee, "Reduced perovskite LaNiO₃ catalysts modified with Co and Mn for low coke formation in dry reforming of methane," *Applied Catalysis A: General*, vol. 575, pp. 198-203, 2019.
- [22] C. A. Grambow, L. Pattanaik, and W. H. Green, "Deep learning of activation energies," *The journal of physical chemistry letters*, vol. 11, no. 8, pp. 2992-2997, 2020.
- [23] N. S. Khan, Z. Shah, M. Shutaywi, P. Kumam, and P. Thounthong, "A comprehensive study to the assessment of Arrhenius activation energy and binary chemical reaction in swirling flow," *Scientific Reports*, vol. 10, no. 1, p. 7868, 2020.
- [24] L. U. Okonye, Y. Yao, J. Ren, X. Liu, and D. Hildebrandt, "A perspective on the activation energy dependence of the Fischer-Tropsch synthesis reaction mechanism," *Chemical engineering science*, vol. 265, p. 118259, 2023.
- [25] S. Das, M. Shah, R. K. Gupta, and A. Bordoloi, "Enhanced dry methane reforming over Ru decorated mesoporous silica and its kinetic study," *Journal of CO₂ Utilization*, vol. 29, pp. 240-253, 2019.
- [26] A. H. Khoja, M. Tahir, N. A. S. Amin, A. Javed, and M. T. Mehran, "Kinetic study of dry reforming of methane using hybrid DBD plasma reactor over La₂O₃ co-supported Ni/MgAl₂O₄ catalyst," *international journal of hydrogen energy*, vol. 45, no. 22, pp. 12256-12271, 2020.
- [27] L. Pino, C. Italiano, M. Laganà, A. Vita, and V. Recupero, "Kinetic study of the methane dry (CO₂) reforming reaction over the Ce 0.70 La 0.20 Ni 0.10 O 2- δ catalyst," *Catalysis Science & Technology*, vol. 10, no. 8, pp. 2652-2662, 2020.